ELSEVIER

Earth and Planetary Science Letters 190 (2001) 221–235

EPSL

www.elsevier.com/locate/epsl

Inherent gravitational instability of thickened continental crust with regionally developed low- to medium-pressure granulite facies metamorphism

Taras V. Gerya [a,b], Walter V. Maresch [b,*], Arne P. Willner [b], Dirk D. Van Reenen [c], C. Andre Smit [c]

[a] *Institute of Experimental Mineralogy, Russian Academy of Sciences, Chernogolovka, Moscow District 142432, Russia*
[b] *Institut für Geologie, Mineralogie und Geophysik, Ruhr-Universität Bochum, 44780 Bochum, Germany*
[c] *Department of Geology, Rand Afrikaans University, Auckland Park, South Africa*

Received 27 September 2000; received in revised form 1 June 2001; accepted 6 June 2001

Abstract

Petrological arguments show that regionally developed low- to medium-pressure, high-temperature granulite facies metamorphism may critically enhance the lowering of crustal density with depth. This leads to gravitational instability of homogeneously thickened continental crust, mainly due to changes in mineral assemblages and the thermal expansion of minerals in conjunction with the exponential lowering of the effective viscosity of rocks with increasing temperature. It is argued that crustal processes of gravitational redistribution (crustal diapirism) contributing to the exhumation of granulite facies rocks may be activated in this way.

Keywords: granulites; density; gravity sliding; crust; diapirism

1. Introduction

Numerous structural, geochronological and petrological studies have recognized tectono-metamorphic processes leading to the formation of granulite complexes within continental crust (see reviews [1–3]). In a review by Harley [1] of about 90 granulite complexes, a remarkable diversity in granulite characteristics, particularly retrograde *P–T* paths, was emphasized. This diversity mirrors the variety of tectonic histories of granulites. Hence no single universal tectonic model for the origin and exhumation of granulites can be advocated [1].

However, while tectonic models of formation of different granulite complexes are diverse, it is widely believed that the driving forces operating during their geodynamic histories were of external nature with respect to the continental crust itself. The most important geodynamic processes considered for the origin of granulites are (see reviews [1–3]): (i) tectonic thickening or thinning of the continental crust, (ii) magmatic underplating (magmatic accretion), (iii) delamination of cold

* Corresponding author. Tel.: +49-234-3228155; Fax: +49-234-3214433.
E-mail address: walter.maresch@ruhr-uni-bochum.de (W.V. Maresch).

0012-821X/01/$ – see front matter
PII: S0012-821X(01)00394-6

mantle lithosphere and (iv) tectonic exhumation of crustal blocks associated with erosion.

In this respect an important addition was made by Perchuk [4], who emphasized the critical role of internal crustal buoyancy forces [5] as a factor for the exhumation of some Precambrian granulite terrains. Because of the exponential decrease in the viscosity of rocks with increasing temperature (e.g. [6,7]), high-grade granulite facies metamorphism could trigger processes of crustal diapirism [4,5] in gravitationally unstable continental crust. The general validity of a gravitational instability model for the exhumation of granulites has been underlined by numerical geodynamic experiments [8], including the numerical modeling of different types of P–T paths [9].

The following major factors for the formation of gravitationally unstable continental crust are discussed in the literature:

1. magmatic processes:
   - the invasion of basic magmas in the form of huge quantities of lava pouring out on the top of continental crust (e.g. plateau basalt) or injected as sills, dykes and plutons within continental crust [5];
   - the presence of mafic and ultramafic volcanic and plutonic rocks within greenstone belts situated in the upper portion of cratonic successions in granite-greenstone belts (e.g. [4,5,8]);
   - the medium-scale (100–4000 m), rhythmic interlayering of rocks of different densities within the crust, leading to the growth of regional diapirs, due to dynamic interaction of low-density rocks during gravitational redistribution processes [8];
2. crustal anatexis and granitization processes:
   - granitoid intrusion, charnockitization and melting related to high-grade metamorphism (e.g. [4,5,10]);
3. tectonic processes:
   - selective thickening of the continental crust in orogenic belts [5];
   - regional stacking of continental crust during collision, creating a potentially unstable thickened crust in areas with initially stable crustal profiles (e.g. double-stacked crust, [11,12]).

This list should be augmented by a consideration of the metamorphic phase transformations that could also control the formation of regional-scale gravitational instabilities during high-temperature, medium-pressure granulite facies metamorphism [13]. Phase transformations are often considered to be a key factor in the increase of the density of crustal rocks with increasing metamorphic grade and depth (e.g. [12,14]). However, the calculations of Bousquet et al. [14] show that medium-pressure, two-pyroxene granulites have a characteristically lower density (by 30–90 kg/m^3) than rocks of the same chemical composition at amphibolite facies grade. Therefore, increasing temperature during prograde granulite metamorphism may actually produce an inversion of rock densities with depth. This could be expected to lead to a regional gravitational instability within an initially stable, homogeneously thickened crust. The relationship between the thermal regime of metamorphism and gravitational instability of the continental crust was not discussed by Bousquet et al. [14] and needs further investigation.

The major purpose of the present paper is to quantify the influence of changes in mineral assemblages and P–V–T properties of metamorphic minerals on crustal density profiles. For this purpose, the Gibbs free energy minimization approach (e.g. [15–17]) is used.

2. Methodology

2.1. Compositional and thermal model

In our study we adopted a commonly used one-dimensional generalized model of homogeneously thickened continental crust [11,12], in which the upper portion is composed of rocks with average granodioritic composition [11,12]. Low- to medium-pressure granulite facies conditions in our model are assumed to be generated in this granodioritic portion of thickened crust at 20–30 km depth. The relatively felsic composition of the

crust undergoing the granulite facies metamorphism is in accordance with existing data for many granulite regions (see review [1]). In contrast to the granulite xenolith population heavily dominated by mafic compositions, the extensive outcrops of granulite terrains are usually dominated by felsic to intermediate orthogneisses and metasediments [1]. As boundary conditions we accepted $T = 25$°C at the Earth's surface and an assumed variable temperature at the boundary between the upper and lower crust at 23–30 km depth. Using these conditions, a set of steady-state temperature profiles (i.e. geotherms) was calculated for the upper crust (Fig. 1a) according to:

$$k(\partial^2 T/\partial z^2) + H_T = 0 \quad (1)$$

where z is depth, m, T is temperature, K, k is thermal conductivity of the medium, W/(m·K), and H_T is radiogenic heat production in the medium, W/m^3. The values of $k = 2.25$ W/(m K) and $H_T = 2{\cdot}10^{-6}$ W/m^3 for the upper crust were taken from [11].

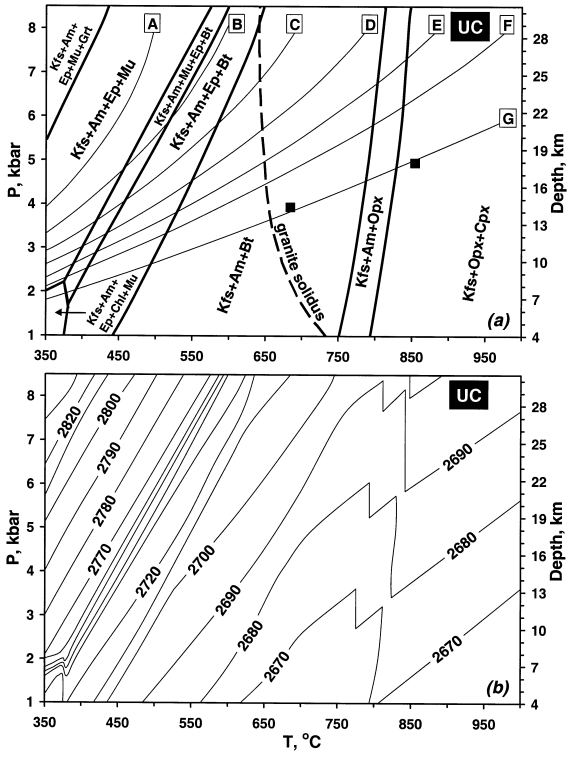

Fig. 1. Petrogenetic grid (a) and density (kg/m^3) map (b) calculated for crust of granodioritic composition (see UC in Table 1). Quartz, plagioclase and Fe–Ti oxides are present in all mineral assemblages. Heavy dashed line in (a) corresponds to H_2O-saturated granite solidus [18]. Geotherms in (a) (thin lines labelled A–G) are calculated using Eq. 1 at different lower boundary conditions: A – 500°C at 30 km, B – 600°C at 30 km, C – 700°C at 30 km, D – 800°C at 30 km, E – 900°C at 30 km, F – 1000°C at 30 km, G – 1000°C at 23 km. Black solid rectangles in (a) show peak metamorphic conditions estimated for granulite [19] and amphibolite [20] zones in the Namaqualand granulite terrain (cf. Fig. 8).

2.2. Calculation of rock density

In contrast to Bousquet et al. [14], who calculated rock densities for idealized mineral assemblages, we used the Gibbs free energy minimization procedure to calculate equilibrium assemblages and compositions of minerals for a given pressure, temperature and rock composition. The density was then calculated as the ratio of the sum of the molar masses to the sum of the molar volumes of the constituent minerals, where each mass and volume is weighted by the mol abundance of the mineral in the rock. In programming the Gibbs free energy minimization procedure we adopted an algorithm suggested by de Capitani and Brown [16] for complex systems containing non-ideal solid solutions. Thermodynamic data for minerals and aqueous fluid were taken from the internally consistent database of Holland and Powell [21]. Mixing models of solid solutions consistent with this database were taken from the literature [21–24]. Two types of calculations were performed: (i) calculation of petrogenetic grids and corresponding density maps with a resolution of 5 K and 100 bar for T and P, respectively, and (ii) calculation of density profiles along geotherms with a resolution of 100 m ($\sim$30 bar). For crustal density profiles, equilibrium assemblages were calculated at temperatures $\geq$300°C. At lower temperatures the assemblages calculated for $T = 300$°C were assumed to be present.

We considered six different types of metamorphic rocks as possible major lithologies for the crust as a whole (Table 1): granodioritic (UC), andesitic (AC) and gabbroic (LC) crust [25], high-grade metapelite (MP) [26], typical Precam-

Table 1
Rock compositions[a] used for density calculations

	UC[b]	LC[b]	AC[b]	KG[b]	MP[b]	FG[b]
SiO_2	66.12	54.48	57.94	65.81	65.30	71.34
TiO_2	0.50	1.00	0.80	0.81	0.81	0.40
Al_2O_3	15.24	16.14	17.94	15.24	17.84	14.57
$Fe_2O_3^c$	1.03	2.42	1.70	1.73	1.61	0.71
FeO	3.39	7.97	5.62	5.71	5.33	2.35
MgO	2.21	6.32	3.50	2.73	2.38	1.11
CaO	4.21	8.52	7.49	2.73	1.27	2.83
Na_2O	3.91	2.81	3.50	2.12	2.02	3.85
K_2O	3.38	0.34	1.50	3.13	3.44	2.83

[a]In wt%, sums of oxides normalized to 100%.
[b]Abbreviations used: UC, LC and AC – upper granodioritic, lower gabbroic and andesitic crust, respectively [25]; MP – typical high-grade metapelite composition [26]; KG – average composition of granulites of the Kanskiy complex (Yenisey Range, Eastern Siberia) [27]; FG – average composition of Precambrian felsic granulites [28].
[c]Fe^{3+} is taken as 25 atomic % from Fe total.

brian granulite (KG) represented by the average composition of the Kanskiy granulite complex, Yenisey Range, Eastern Siberia [27], and the average composition of Archean felsic granulites (FG) [28]. Molar abundances of minerals were calculated from bulk rock compositions (Table 1) using a system of mass-balance equations for 10 components: SiO_2, TiO_2, Al_2O_3, MgO, Fe_2O_3, FeO, CaO, Na_2O, K_2O and H_2O. To avoid unrealistic mineral assemblages, cordierite, andalusite and sillimanite had to be considered as unstable in clinopyroxene-normative rocks (UC, AC, LC, FG). For the same reason, calcic amphibole and clinopyroxene were considered unstable in Al-rich metapelites (MP). The system was considered to be open for H_2O [14], i.e. the volatiles produced in dehydration reactions are assumed to be removed. Therefore, although fluid phase saturation was ensured for all calculated equilibrium mineral assemblages such fluids were not involved in density calculations. P–T-dependent volumes of phases, V, in equilibrium mineral assemblages were calculated via the Gibbs potential, G, using the thermodynamic relation $V=\partial G/\partial P$ and a numerical differentiation procedure.

The influence of partial melting on gravitational instability of the crust has been studied theoretically using numerical geodynamic modeling (e.g. [10]). In our study we have concentrated on melt-absent conditions typical for many granulite facies terrains. In order to simulate these conditions, a lowered water activity was assumed at temperatures above 630°C (cf. granite solidus in Fig. 1a) according to the following empirical equation:

$$a_{H_2O}=1.0-[(T_K+20-t_1)/(t_2-t_1)1.2]^{0.865} \quad (2)$$

where $t_1=877+160/(P_{kbar}+0.348)^{0.75}$ and $t_2=1262+9P_{kbar}$, $0.1<a_{H_2O}<1.0$. Eq. 2 was calibrated using data on the P–T parameters of the granite solidus calculated for different a_{H_2O} [18]. This equation allows the granite melting temperature to be constrained at 20 K above the given temperature T_K for a given pressure P_{kbar} and provides a transition to the conditions of granulite facies metamorphism characterized by lowered water activity [1–3].

3. Results of density calculations

Simplified petrogenetic grids and corresponding density maps obtained for the rocks studied (Table 1) are presented in Figs. 1–3 and examples of calculated crustal density profiles are shown in Fig. 4. Examples of calculated mineral assemblages for specific P–T conditions are presented in Table 2 (see **Background Dataset**[1]). Abbreviations of mineral names are after Kretz [29].

[1] http://www.elsevier.com/locate/epsl

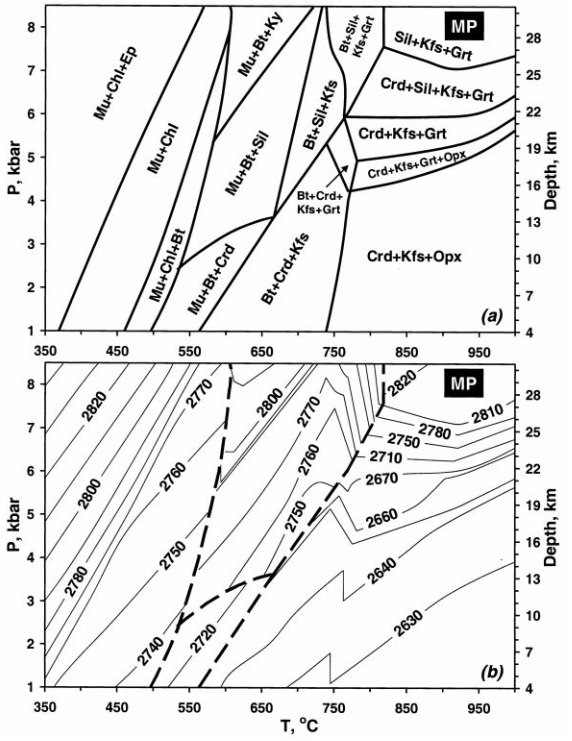

Fig. 2. Petrogenetic grid (a) and density (kg/m^3) map (b) calculated for typical high-grade metapelite (see MP in Table 1). Quartz, plagioclase and Fe–Ti oxides are present in all mineral assemblages. Heavy dashed lines in (b) mark particularly abrupt changes in density related to differences in mineral assemblage.

3.1. Influence of changes in mineral assemblages

Figs. 1–3 show that the density generally decreases toward lower pressures and higher temperatures for all types of rocks. The maximum densities are characteristic for greenschist and in part low-grade amphibolite facies rocks and the minimum densities are obtained for high-grade amphibolite and granulite facies rocks of low to moderate pressure. The decrease in density with increase in metamorphic grade is mainly related to reactions producing anorthite-rich plagioclase (instead of epidote), sillimanite (instead of kyanite) and cordierite. This causes a significant (40–150 kg/m^3) decrease in crustal density with depth for high-temperature geotherms characterized by low dP/dT gradients (Fig. 4). This decrease represents the combined influence of both the P–V–T properties of individual minerals as well as metamorphic reactions. The isolated effects of metamorphic phase transformations, represented by changes in the standard (at $T = 25$°C and $P = 1$ bar) density of different mineral assemblages, vary from 20 to 80 kg/m^3.

3.2. Influence of the P–V–T properties of minerals

The influence of the P–V–T properties of individual minerals on crustal density profiles was isolated by calculating densities of minerals and of rocks with fixed mineral compositions along the geotherms shown in Fig. 1a using the P–V–T equations of Berman [30], Gerya et al. [31] and Holland and Powell [21]. The results indicate that along geotherms with relatively low dP/dT gradients (e.g. geotherms C–G in Fig. 1a) the density of rock-forming minerals decreases with depth. The most significant decrease (40–90 kg/m^3) is characteristic for Fe–Mg silicates and quartz, while for feldspars this effect is less prominent (10–40 kg/m^3). Density profiles calculated for granodioritic crust of constant mineral composition (such as assemblage Kfs+Opx+Cpx in Fig. 1) indicate that the changes in density induced by the P–V–T properties of individual minerals (20–50 kg/m^3) are smaller than, but of the same direction and order of magnitude as those caused by changes in mineral assemblages (20–80 kg/m^3).

3.3. Influence of continuous metamorphic reactions

Most changes in the mineral assemblages of metamorphic rocks proceed via transitional high-variance assemblages. In the case of dehydration reactions, the stability fields of these assemblages may be relatively narrow (≤ 10 K), defining abrupt changes in density with increasing temperature (cf. the transition between Kfs+Am+Opx and Kfs+Opx+Cpx assemblages in Fig. 1a). On the other hand, transitional assemblages can be stable over a wide range of pressure (1–2 kbar) and temperature (50–100 K), providing relatively smooth changes in density (cf. the density distribution within the Crd+Sil+Kfs+Grt assemblage in Fig. 2). In both cases, the variation in density of a rock is related to systematic changes

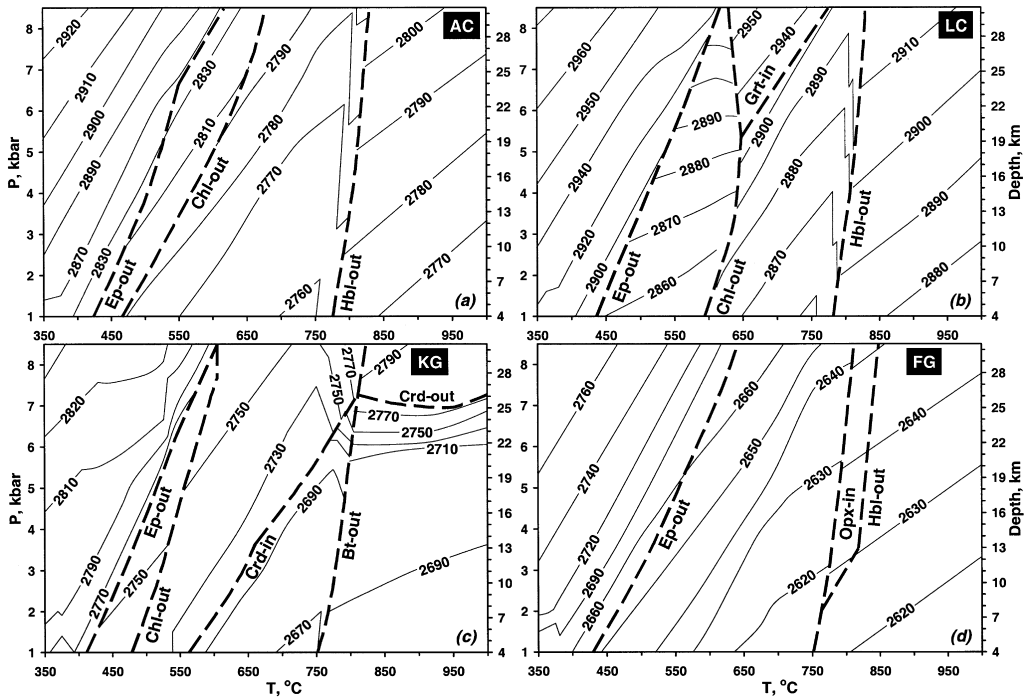

Fig. 3. Density (kg/m^3) maps calculated for crust of andesitic (a) and gabbroic (b) composition (see AC and LC in Table 1), as well as the average compositions of the Kanskiy granulite complex (c) and Precambrian felsic granulites (d) (see KG and FG in Table 1). Heavy dashed lines indicate important changes in mineral assemblages.

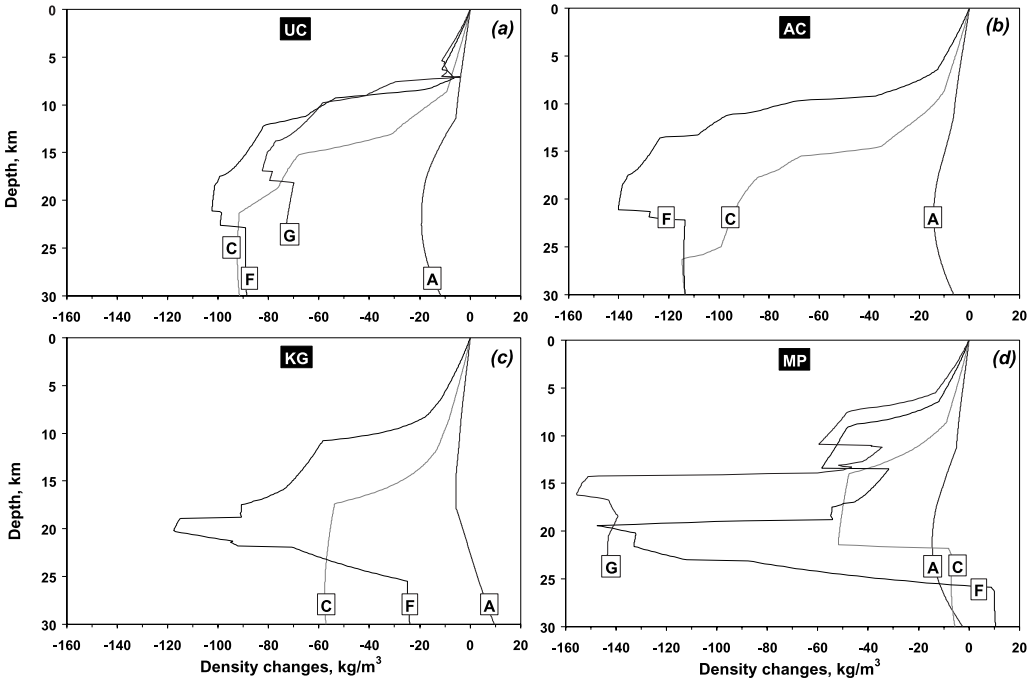

Fig. 4. Typical examples of density profiles calculated along the geotherms shown in Fig. 1a.

in the modal amounts of the constituent minerals with changing P and T.

4. Geodynamic implications

4.1. Degree of potential gravitational instability of the crust

On the basis of the results presented above, it can be concluded that in cases of vertical metamorphic zoning related to low- to medium-pressure granulite facies metamorphism, a considerable (50–150 kg/m^3) decrease in density of rocks should be a rather common feature in the lower levels of upper crust of relatively homogeneous composition. This should be especially characteristic for crust of felsic to intermediate composition. In order to quantify this phenomenon in terms of gravitational energy, we used a set of density profiles calculated for crust of different composition along different geotherms (Fig. 4). Fig. 4 shows that a zone of lowered density could appear in thickened upper crust when the temperature at its base exceeds 600–700°C. For temperatures exceeding 800°C, which is typical for medium- to low-pressure granulite facies conditions (e.g. [1]), the thickness of the low-density layer could reach 5–15 km, providing a high degree of internal gravitational instability for the thickened crust.

This degree can be quantified in terms of the maximum internal gravitational energy that can be released by gravitational redistribution. For any given density profile, this value can be estimated by comparison to a gravitationally stable 'ordered' profile, in which the volume ratios of rocks with various densities are equivalent but the density of crust does not decrease with depth. The following equation can then be used to calculate the maximum internal gravitational energy of the crust:

$$U = g/h \int_{z=a}^{h} [\rho(z) - \rho_o(z)](h-z)\mathrm{d}z \qquad (3)$$

where U is mean gravitational energy, J/m^3; $h = 30\,000$ m is thickness of the upper crust; $\rho(z)$ and $\rho_o(z)$ are calculated and theoretical 'ordered' density profiles with depth z, respectively; $g = 9.81$ m/s^2 is acceleration within the gravity field; a is the depth for $T = 400$°C ($\sim$lower limit of greenschist facies [26]). To avoid overestimation of gravitational energy caused by the possible presence of non- or only partially metamorphosed rocks in the upper portion of the crust at temperatures < 400°C, 'ordering' of calculated density profiles was only considered in the a–h depth interval.

Fig. 5a shows the gravitational energy of 30 km of thickened upper crust as a function of temperature at its base. For most of the model crustal compositions the degree of gravitational instability increases strongly within the temperature interval 600–800°C, which corresponds to high-grade amphibolite and granulite facies conditions. For crust of pelitic composition this increase is shifted to higher temperatures of 800–1000°C, this is related to the stability of low-density, cordierite-bearing assemblages (Fig. 2).

The gravitational energy can be compared with the average calculated enthalpy (Fig. 5b) for rocks along different geotherms. The enthalpy of a rock was calculated as the sum of the molar enthalpies of the constituent minerals, weighted by the molar abundance of minerals in the rock. The increase in the average enthalpy (Fig. 5b) reflects the increase in the thermal energy of the crust. From Fig. 5 it follows that the calculated increase in gravitational energy of the crust is $\sim$three orders of magnitude less than the increase in its thermal energy. Thus, the production of gravitational instability within the crust during high-temperature metamorphism requires a negligible part of the thermal energy and does not affect the general balance of heat within the crust.

4.2. The effect of viscosity

The possibility of gravitational redistribution in an unstable crust is greatly dependent on its effective viscosity. The viscosity of crustal rocks decreases exponentially with increasing temperature (e.g. [6,7]) and therefore varies significantly with depth, depending on the geothermal gradient. In Fig. 6 the viscosity of quartz-bearing rocks common in granulite facies terrains has been calcu-

Table 2
Selected calculations of equilibrium mineral assemblages and densities of rocks from Table 1

UC (granodioritic)				
	UC1	UC2	UC3	UC4
T (°C)/P (kbar)	400/2.46	500/3.61	700/4.89	850/6.38
Facies	Greenschist	Amphibolite low-grade	Amphibolite high-grade	Granulite
Relative molar abundance of minerals (mol)	Qtz = 24.21 Kfs = 2.89 Rt = 0.41 Ms = 0.81 $KFe_{0.32}Mg_{0.08}Al_{2.20}Si_{3.40}O_{10}(OH)_2$ Pl = 9.02 $Ca_{0.15}Na_{0.85}Al_{1.15}Si_{2.85}O_8$ Bt = 1.00 $KFe_{1.17}Mg_{1.81}Al_{1.04}Si_{2.98}O_{10}(OH)_2$ Ep = 1.21 $Ca_2Fe_{0.69}Al_{2.31}Si_3O_{12}(OH)$ Am = 0.57 $Na_{0.99}Ca_2Fe_{1.92}Mg_{2.98}Al_{1.19}Si_{6.91}O_{22}(OH)_2$	Qtz = 23.32 Kfs = 4.21 Rt = 0.41 Mag = 0.42 Pl = 10.54 $Ca_{0.30}Na_{0.70}Al_{1.30}Si_{2.70}O_8$ Bt = 0.48 $KFe_{1.14}Mg_{1.82}Al_{1.08}Si_{2.96}O_{10}(OH)_2$ Am = 0.88 $Na_{0.97}Ca_2Fe_{1.76}Mg_{3.09}Al_{1.27}Si_{6.88}O_{22}(OH)_2$	Qtz = 23.25 Kfs = 4.21 Rt = 0.41 Mag = 0.42 Pl = 10.56 $Ca_{0.30}Na_{0.70}Al_{1.30}Si_{2.70}O_8$ Bt = 0.48 $Fe_{1.16}Mg_{1.80}Al_{1.08}Si_{2.96}O_{10}(OH)_2$ Am = 0.87 $Na_{0.95}Ca_2Fe_{1.76}Mg_{3.10}Al_{1.23}Si_{6.91}O_{22}(OH)_2$	Qtz = 19.49 Kfs = 4.70 Rt = 0.18 Mag = 0.42 Ilm = 0.23 Pl = 11.48 $Ca_{0.28}Na_{0.72}Al_{1.28}Si_{2.72}O_8$ Opx = 1.92 $Fe_{0.75}Mg_{1.23}Al_{0.04}Si_{1.98}O_6$ Cpx = 1.67 $CaFe_{0.25}MgO_{0.73}Al_{0.04}Si_{1.98}O_6$
ρ_o (kg/m^3)[a]	2758	2721	2721	2734
ρ_l (kg/m^3)[a]	2742	2698	2682	2693
AC (Andesitic)				
	AC1	AC2	AC3	AC4
T (°C)/P (kbar)	400/2.46	500/3.61	700/4.89	850/6.38
Facies	Greenschist	Amphibolite low-grade	Amphibolite high-grade	Granulite
Relative molar abundance of minerals (mol)	Qtz = 16.98 Rt = 0.66 Ms = 2.11 $KFe_{0.28}Mg_{0.07}Al_{2.30}Si_{3.35}O_{10}(OH)_2$ Pl = 7.84 $Ca_{0.20}Na_{0.80}Al_{1.20}Si_{2.80}O_8$ Ep = 2.48 $Ca_2Fe_{0.57}Al_{2.43}Si_3O_{12}(OH)$ Chl = 0.72 $Fe_{1.89}Mg_{3.10}Al_{2.02}Si_{2.99}O_{10}(OH)_8$ Am = 1.16 $Na_{0.99}Ca_2Fe_{1.96}Mg_{2.89}Al_{1.29}Si_{6.86}O_{22}(OH)_2$	Qtz = 18.34 Rt = 0.66 Mag = 0.33 Ep = 0.91 $Ca_2Fe_{0.82}Al_{2.18}Si_3O_{12}(OH)$ Bt = 2.11 $KFe_{1.20}Mg_{1.75}Al_{1.10}Si_{2.95}O_{10}(OH)_2$ Pl = 12.33 $Ca_{0.45}Na_{0.55}Al_{1.45}Si_{2.55}O_8$ Am = 0.71 $Na_{0.97}Ca_2Fe_{1.92}Mg_{2.86}Al_{1.40}Si_{6.81}O_{22}(OH)_2$	Qtz = 17.25 Kfs = 0.84 Rt = 0.66 Mag = 0.70 Pl = 12.89 $Ca_{0.51}Na_{0.49}Al_{1.51}Si_{2.49}O_8$ Bt = 1.27 $KFe_{1.17}Mg_{1.78}Al_{1.10}Si_{2.95}O_{10}(OH)_2$ Am = 1.15 $Na_{0.93}Ca_2Fe_{1.77}Mg_{3.02}Al_{1.35}Si_{6.86}O_{22}(OH)_2$	Qtz = 10.57 Kfs = 2.11 Rt = 0.28 Mag = 0.70 Ilm = 0.38 Pl = 14.10 $Ca_{0.47}Na_{0.53}Al_{1.47}Si_{2.53}O_8$ Cpx = 2.15 $CaFe_{0.25}Mg_{0.72}Al_{0.06}Si_{1.97}O_6$ Opx = 3.43 $Fe_{0.76}Mg_{1.21}Al_{0.06}Si_{1.97}O_6$
ρ_o (kg/m^3)[a]	2892	2826	2809	2835
ρ_l (kg/m^3)[a]	2874	2801	2771	2795
LC (gabbroic)				
	LC1	LC2	LC3	LC4
T (°C)/P (kbar)	400/2.46	500/3.61	700/4.89	850/6.38
Facies	Greenschist	Amphibolite low-grade	Amphibolite high-grade	Granulite
Relative molar abundance of minerals (mol)	Qtz = 17.43 Rt = 0.82 Ms = 0.47 $KFe_{0.28}Mg_{0.08}Al_{2.28}Si_{3.36}O_{10}(OH)_2$ Pl = 5.60 $Ca_{0.18}Na_{0.82}Al_{1.18}Si_{2.82}O_8$ Ep = 3.12 $Ca_2Fe_{0.63}Al_{2.37}Si_3O_{12}(OH)$ Chl = 1.91 $Fe_{1.77}Mg_{3.22}Al_{2.02}Si_{2.99}O_{10}(OH)_8$ Am = 1.31 $Na_{0.99}Ca_2Fe_{1.82}Mg_{3.05}Al_{1.25}Si_{6.88}O_{22}(OH)_2$	Qtz = 18.58 Rt = 0.82 Mag = 0.98 Pl = 9.14 $Ca_{0.59}Na_{0.41}Al_{1.59}Si_{2.41}O_8$ Chl = 0.71 $Fe_{1.44}Mg_{3.52}Al_{2.08}Si_{2.96}O_{10}(OH)_8$ Bt = 0.47 $KFe_{1.00}Mg_{1.89}Al_{1.22}Si_{2.89}O_{10}(OH)_2$ Am = 2.23 $Na_{0.96}Ca_2Fe_{1.53}Mg_{3.06}Al_{1.78}Si_{6.63}O_{22}(OH)_2$	Qtz = 15.22 Rt = 0.21 Ilm = 0.61 Mag = 0.98 Pl = 10.56 $Ca_{0.60}Na_{0.40}Al_{1.60}Si_{2.40}O_8$ Bt = 0.47 $KFe_{0.82}Mg_{2.06}Al_{1.24}Si_{2.88}O_{10}(OH)_2$ Opx = 2.48 $Fe_{0.76}Mg_{1.19}Al_{0.10}Si_{1.95}O_6$ Am = 1.78 $Na_{0.90}Ca_2Fe_{1.14}Mg_{3.51}Al_{1.60}Si_{6.75}O_{22}(OH)_2$	Qtz = 8.05 Kfs = 0.47 Mag = 0.98 Rt = 0.82 Pl = 12.69 $Ca_{0.54}Na_{0.46}Al_{1.54}Si_{2.46}O_8$ Opx = 6.16 $Fe_{0.69}Mg_{1.28}Al_{0.06}Si_{1.97}O_6$ Cpx = 3.05 $CaFe_{0.22}MgO_{0.75}Al_{0.06}Si_{1.97}O_6$
ρ_o (kg/m^3)[a]	2943	2898	2927	2952
ρ_l (kg/m^3)[a]	2925	2873	2886	2908

Table 2 (*continued*)

MP (metapelitic)				
	MP1	MP2	MP3	MP4
T (°C)/P (kbar)	400/2.46	500/3.61	700/4.89	850/6.38
Facies	Greenschist	Amphibolite low-grade	Amphibolite high-grade	Granulite
Relative molar abundance of minerals (mol)	Qtz = 37.37 Rt = 0.68 Mag = 0.66 Pl = 5.76 $Ca_{0.24}Na_{0.76}Al_{1.24}Si_{2.76}O_8$ Chl = 1.35 $Fe_{2.11}Mg_{2.84}Al_{2.10}Si_{2.95}O_{10}(OH)_8$ Ms = 4.90 $KFe_{0.12}Mg_{0.03}Al_{2.70}Si_{3.15}O_{10}(OH)_2$ Ep = 0.06 $Ca_2Fe_{0.68}Al_{2.32}Si_3O_{12}(OH)$	Qtz = 38.19 Rt = 0.68 Mag = 0.68 Pl = 5.88 $Ca_{0.26}Na_{0.74}Al_{1.26}Si_{2.74}O_8$ Chl = 1.21 $Fe_{2.06}Mg_{2.76}Al_{2.36}Si_{2.82}O_{10}(OH)_8$ Ms = 4.52 $KFe_{0.09}Mg_{0.03}Al_{2.76}Si_{3.12}O_{10}(OH)_2$ Bt = 0.38 $KFe_{1.26}Mg_{1.32}Al_{1.84}Si_{2.58}O_{10}(OH)_2$	Qtz = 38.77 Kfs = 2.06 Sil = 4.39 Rt = 0.68 Mag = 0.68 Pl = 5.88 $Ca_{0.26}Na_{0.74}Al_{1.26}Si_{2.74}O_8$ Bt = 2.84 $KFe_{1.19}Mg_{1.39}Al_{1.84}Si_{2.58}O_{10}(OH)_2$	Qtz = 28.71 Kfs = 4.90 Sil = 0.91 Rt = 0.68 Mag = 0.68 Pl = 5.80 $Ca_{0.25}Na_{0.75}Al_{1.25}Si_{2.75}O_8$ Grt = 1.33 $Ca_{0.06}Fe_{1.87}Mg_{1.07}Al_2Si_3O_{12}$ Crd = 1.70 $Fe_{0.52}Mg_{1.48}Al_4Si_5O_{18}(H_2O)_{0.39}$
ρ_o (kg/m^3)[a]	2772	2771	2794	2752
ρ_1 (kg/m^3)[a]	2755	2744	2747	2717
FG (average felsic granulite)				
	FG1	FG2	FG3	FG4
T (°C)/P (kbar)	400/2.46	500/3.61	700/4.89	850/6.38
Facies	Greenschist	Amphibolite low-grade	Amphibolite high-grade	Granulite
Relative molar abundance of minerals (mol)	Qtz = 34.84 Kfs = 1.51 Rt = 0.33 Pl = 9.24 $Ca_{0.14}Na_{0.86}Al_{1.14}Si_{2.86}O_8$ Ms = 1.73 $KFe_{0.33}Mg_{0.08}Al_{2.18}Si_{3.41}O_{10}(OH)_2$ Ep = 0.82 $Ca_2Fe_{0.71}Al_{2.29}Si_3O_{12}(OH)$ Bt = 0.68 $KFe_{1.21}Mg_{1.77}Al_{1.04}Si_{2.98}O_{10}(OH)_2$ Am = 0.17 $Na_{0.99}Ca_2Fe_{2.07}Mg_{2.82}Al_{1.21}Si_{6.90}O_{22}(OH)_2$	Qtz = 34.76 Kfs = 2.84 Rt = 0.33 Mag = 0.29 Pl = 11.33 $Ca_{0.29}Na_{0.71}Al_{1.29}Si_{2.71}O_8$ Bt = 1.08 $KFe_{1.32}Mg_{1.64}Al_{1.08}Si_{2.96}O_{10}(OH)_2$ Am = 0.01 $Na_{0.98}Ca_2Fe_{2.22}Mg_{2.61}Al_{1.32}Si_{6.85}O_{22}(OH)_2$	Qtz = 34.76 Kfs = 2.91 Rt = 0.10 Ilm = 0.23 Mag = 0.29 Pl = 11.33 $Ca_{0.29}Na_{0.71}Al_{1.29}Si_{2.71}O_8$ Bt = 1.00 $KFe_{1.20}Mg_{1.76}Al_{1.08}Si_{2.96}O_{10}(OH)_2$ Am = 0.01 $Na_{0.95}Ca_2Fe_{1.83}Mg_{3.02}Al_{1.25}Si_{6.90}O_{22}(OH)_2$	Qtz = 31.81 Kfs = 3.91 Ilm = 0.33 Mag = 0.29 Pl = 11.35 $Ca_{0.29}Na_{0.71}Al_{1.29}Si_{2.71}O_8$ Opx = 1.47 $Fe_{0.76}Mg_{1.22}Al_{0.04}Si_{1.98}O_6$ Cpx = 0.01 $CaFe_{0.25}MgO_{0.73}Al_{0.04}Si_{1.98}O_6$
ρ_o (kg/m^3)[a]	2721	2676	2676	2685
ρ_1 (kg/m^3)[a]	2704	2652	2633	2641
KG (average Kanskiy granulite)				
	KG1	KG2	KG3	KG4
T (°C)/P (kbar)	400/2.46	500/3.61	700/4.89	850/6.38
Facies	Greenschist	Amphibolite low-grade	Amphibolite high-grade	Granulite
Relative molar abundance of minerals (mol)	Qtz = 36.00 Rt = 0.67 Mag = 0.20 Pl = 5.18 $Ca_{0.13}Na_{0.87}Al_{1.13}Si_{2.87}O_8$ Bt = 0.68 $KFe_{1.23}Mg_{1.75}Al_{1.04}Si_{2.98}O_{10}(OH)_2$ Ep = 1.27 $Ca_2Fe_{0.81}Al_{2.19}Si_3O_{12}(OH)$ Chl = 1.03 $Fe_{2.05}Mg_{2.94}Al_{2.02}Si_{2.99}O_{10}(OH)_8$ Ms = 3.71 $KFe_{0.31}Mg_{0.07}Al_{2.24}Si_{3.38}O_{10}(OH)_2$	Qtz = 39.95 Rt = 0.67 Mag = 0.72 Pl = 7.73 $Ca_{0.42}Na_{0.58}Al_{1.42}Si_{2.58}O_8$ Bt = 2.93 $KFe_{1.17}Mg_{1.51}Al_{1.64}Si_{2.68}O_{10}(OH)_2$ Ms = 1.46 $KFe_{0.10}Mg_{0.03}Al_{2.74}Si_{3.13}O_{10}(OH)_2$	Qtz = 39.55 Sil = 0.93 Kfs = 1.28 Rt = 0.67 Mag = 0.72 Pl = 7.73 $Ca_{0.42}Na_{0.58}Al_{1.42}Si_{2.58}O_8$ Bt = 3.11 $KFe_{1.15}Mg_{1.44}Al_{1.82}Si_{2.59}O_{10}(OH)_2$	Qtz = 30.06 Kfs = 4.39 Rt = 0.67 Mag = 0.72 Pl = 7.61 $Ca_{0.41}Na_{0.59}Al_{1.41}Si_{2.59}O_8$ Opx = 2.03 $Fe_{0.72}Mg_{1.12}Al_{0.32}Si_{1.84}O_6$ Crd = 0.40 $Fe_{0.41}Mg_{1.59}Al_4Si_5O_{18}(H_2O)_{0.39}$ Grt = 1.20 $Ca_{0.09}Fe_{1.61}Mg_{1.30}Al_2Si_3O_{12}$
ρ_o (kg/m^3)[a]	2806	2775	2768	2797
ρ_1 (kg/m^3)[a]	2789	2748	2721	2755

[a] ρ_o is standard density at 298 K and 1 bar (i.e. without P–V–T contribution of individual phases), ρ_1 is density at T and P given.

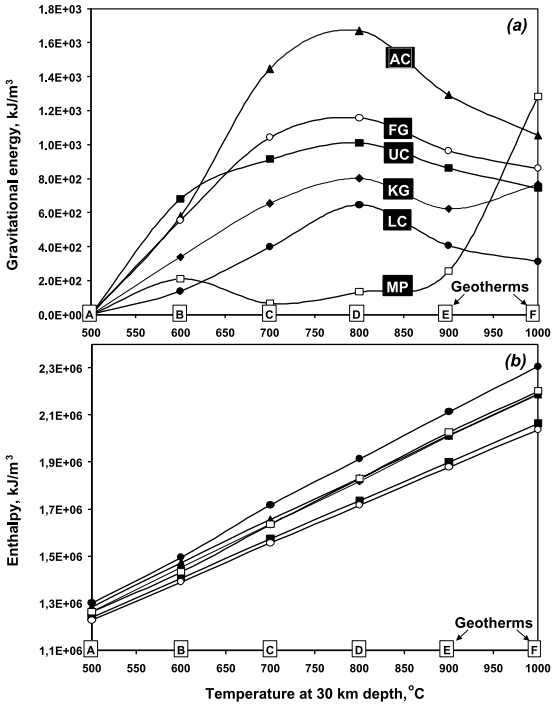

Fig. 5. Gravitational energy (a) and average enthalpy (b) of 30 km of thickened upper crust of various bulk compositions (Table 1) as a function of temperature at its base. Lettering of geotherms as in Fig. 1a.

lated along different geotherms, using experimentally calibrated rheological equations written in the form [7]:

$$\varepsilon = A_{\mathrm{D}}\sigma^{n} \exp\left(-E/RT\right) \tag{4}$$

$$\eta = 10^{6}\sigma/(2\varepsilon) \tag{5}$$

where η is viscosity, Pa s, ε is strain rate, s^{-1}, σ is stress, MPa, E is activation energy, kJ/mol, A_{D} is material constant, MPa^{-n}/s, n is a power-law constant and R is the gas constant. Parameters for Eq. 4 for some minerals and rocks were taken from the summary by Ranalli [7]. In our calculation we used a moderate value for the strain rate of 10^{-14} s^{-1} (e.g. [7,34]). From the data of Fig. 6 it follows that low dP/dT geotherms are characterized by a strong (two to four orders of magnitude) decrease in viscosity at the bottom of thickened upper crust for all rock types considered, forming a rheologically weak zone (e.g. [7,34]). Further decreases in viscosity of high-grade rocks could also be related to partial melting (e.g. [10]) or to the local (e.g. within shear zones) presence of water-bearing fluids (compare results for dry and wet granite and quartzite in Fig. 6a,b). In the case of a gravitational redistribution process the strain rate could vary significantly in time and space (e.g. [10]), thus affecting the effective viscosity of rocks. Although the viscosity profiles shown in Fig. 6 are therefore not suitable for the direct estimation of effective viscosity of rocks during crustal diapirism, it can be argued that a high (10–1000) viscosity contrast between upper (cool and strong) and lower (hot and weak) portions of the crust should be a rather common feature of granulite facies metamorphism. In such a case the development of a crustal-scale gravitational redistribution process would be defined by the effective viscosity of relatively strong low-grade rocks in the upper portion of the crust [5].

4.3. Time-scale estimates

To estimate semi-quantitatively the possible rates of gravitational redistribution as a function

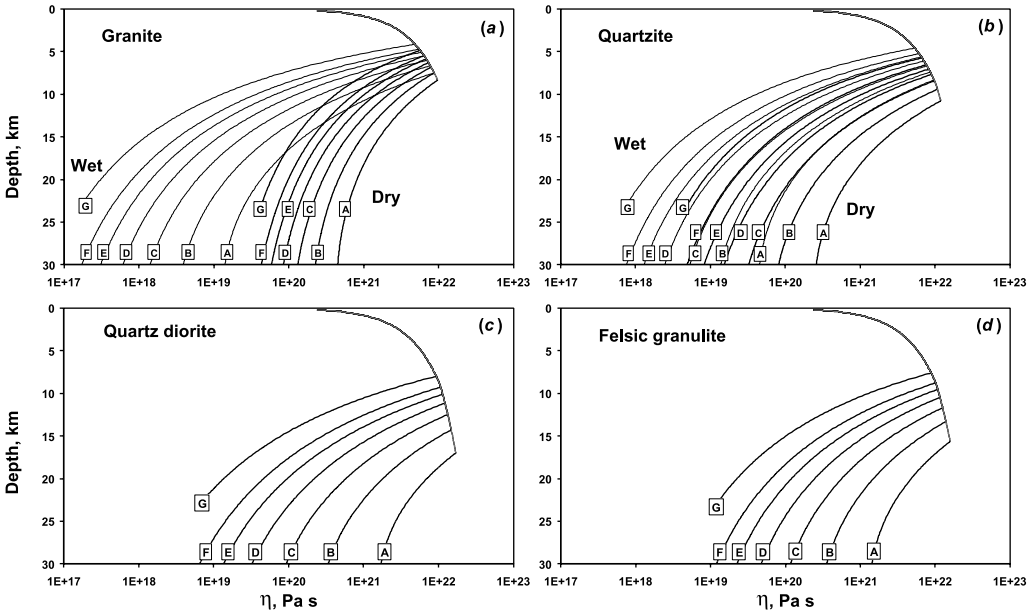

Fig. 6. Viscosity of some quartz-bearing rocks calculated along the geotherms of Fig. 1a at a strain rate of 10^{-14} s^{-1} from the experimentally determined rheological parameters given in [7]. The thick gray line limiting the viscosity profiles denotes the brittle–ductile transition calculated as 'Mohr–Coulomb viscosity' [32] at a strain rate of 10^{-14} s^{-1} after Byerlee's law [33].

of the effective viscosity of the upper (low-grade) portion of the crust, a simple model proposed by Ramberg [5] can be used (Fig. 7a). It is assumed that along a low dP/dT geotherm (e.g. geotherms C–F in Fig. 1a) an inverted step-like distribution of density with depth is characteristic (see Fig. 4a). This distribution can be approximated by a two-layer model with an initial geometry and with boundary conditions as shown in Fig. 7a. A lower non-slip boundary condition is assumed at the bottom of the homogeneous crust. An upper non-slip boundary condition is assumed at an arbitrary level suggested by the significant increase in viscosity with decreasing depth (Fig. 6a,b). It is also assumed that the initial sinusoidal disturbance of the boundary between the two layers of different density within the crust is of small amplitude (A) and characteristic wavelength (λ) [5]. This provides conditions for investigating the growth of the diapir as defined [5] by the equation:

$$y = A \exp\left[t\cdot(\rho_2-\rho_1)\cdot K\cdot H\cdot g/(2\eta_2)\right] \quad (6)$$

where y is the height of the diapir, m; t is time, s; H is the thickness of each layer, m; η_2 is the viscosity of the diapir, Pa s; K is the factor of growth [5] depending on viscosity contrast. Taking into account the calculated density profiles (e.g. Fig. 4a), $H = 10\,000$ m and $(\rho_2-\rho_1) = 100$ kg/m^3 were accepted and A was taken to be 500 m. According to the calculated variations of viscosity with depth (Fig. 6), a high viscosity contrast of $\eta_1/\eta_2 = 10$–500 was used for estimation of $K = 0.032$ ($\eta_1/\eta_2 = 10$) and $K = 0.00065$ ($\eta_1/\eta_2 = 500$) [5]. Fig. 7b shows the height of the diapir as a function of time for different values of η_1 and η_1/η_2. According to these results, a process of gravitational redistribution driven by instabilities induced by phase transformations and thermal expansion of minerals would proceed in realistic time scales on the order of 10–50 Myr at a viscosity of the upper low-grade portion of the crust on the order of 10^{20}–10^{21} Pa s.

Therefore, the initiation of the crustal-scale process of gravitational redistribution requires a lowering of the viscosity of low-grade rocks to 10^{20}–10^{21} Pa s, which could be achieved by the simultaneous influence of an increase in temperature, tectonic stress and fluid/melt activity during

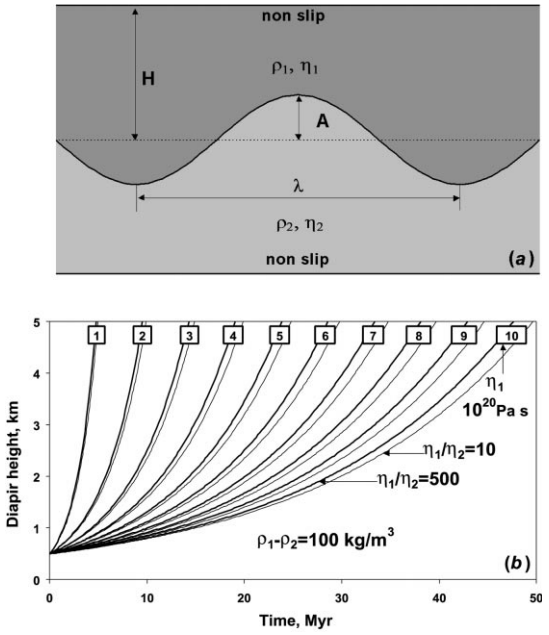

Fig. 7. Modeled diapir growth for a two-layered case [5]. (a) Initial design of the model and boundary conditions. (b) The height of a diapir as a function of time calculated using Eq. 6 at $\eta_1/\eta_2 = 10$ (thin lines) and $\eta_1/\eta_2 = 500$ (thick lines).

the prograde stage of high-grade metamorphism. On the other hand, in the case of weak zones cutting through the upper crust, the rate of gravitational redistribution could be much higher. For example, for the process of fast (within about 9 Myr) buoyant uplift of medium-pressure granulites along a weak tectonic zone, moderate values of the effective viscosity of upper crustal low-grade rocks (10^{21} Pa s) and granulites (10^{19} Pa s) were estimated using the shapes of retrograde *P–T* paths of metapelites from the Limpopo high-grade terrain [9].

5. Discussion and possible geological examples

As follows from Figs. 1–4 the decrease in density of major rock types with depth should be a rather common feature in crust with low- to medium-pressure, high-temperature metamorphism. However, the actual formation of gravitationally unstable density profiles within continental crust will also depend on the evolution of the geothermal gradient, on changes in chemical composition of the crust with depth and on the kinetics of metamorphic phase transformations (especially in the upper low-grade portion of the crust, in which a high-density layer can form). Furthermore, possible gravitational redistribution will depend on the evolution of the degree of gravitational instability and the effective rheology of the crust during and after high-grade metamorphism. It can be argued that the gravitational instability of the crust related to metamorphic phase transformations may in many respects be similar to the instability induced by partial melting of the crust (e.g. [10]). For high-grade metamorphic complexes, both sources of instability should be considered as an important factor that may crucially affect the dynamics of exhumation of high-grade rocks.

A mechanism of buoyant exhumation of granulites driven by the lithological difference between upper and lower crustal rocks has already been suggested for several medium-pressure Precambrian granulite complexes, i.e. the Limpopo granulite complex in South Africa [35], the Lapland complex in the Kola Peninsula [35], the Sharizhalgay complex in the Baikal area, Eastern Siberia [4], the Kanskiy granulite complex in the Yenisey Range, Eastern Siberia [36]. Considering the relatively felsic bulk composition of these complexes (e.g. KG in Table 1), metamorphic phase transformations should be considered to be an additional factor, thus increasing the degree of gravitational instability of the crust during high-temperature, medium-pressure metamorphism.

An excellent example of an extensive low-pressure granulite terrain characterized by an extremely low d*P*/d*T* gradient (compare geotherm G in Fig. 1a) may be found in the Namaqua Mobile Belt of the NW Cape province of South Africa. This granulite terrain of the Bushmanland Subprovince is exposed as a long-wavelength, E–W-trending, dome-like structure of 150–180 km width (Fig. 8), gradually passing into upper amphibolite facies rocks that overly the granulites to the N and S [19,37]. The boundary between both facies areas is the cordierite+garnet+K-feldspar+sillimanite-in-isograd. The granulite and the overlying amphibolite terrains are of similar over-

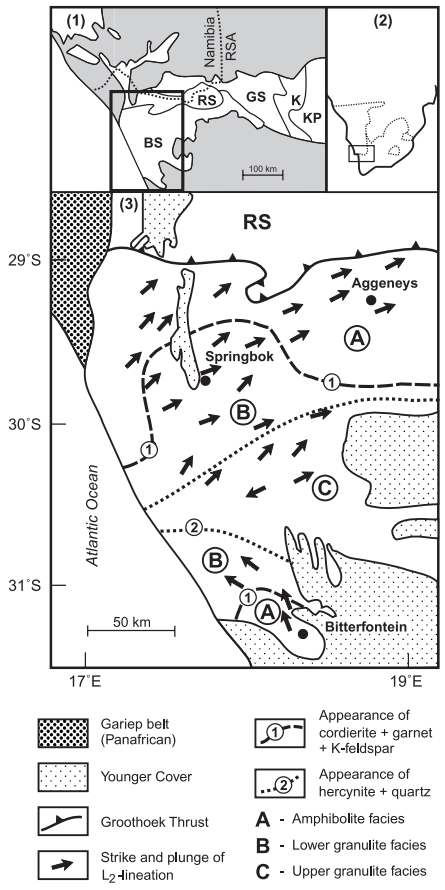

Fig. 8. Structural–metamorphic characteristics of the Namaqualand granulite complex. Abbreviations: BS – Bushmanland Subprovince, RS – Richersvelt Subprovince, GS – Gordonia Subprovince, K – Kheis Belt, KP – Kaapvaal Craton.

all rock composition, dominated chiefly by quartz–feldspar gneisses, minor metapelites and quartzites, as well as subordinate metabasites and iron formations, thus indicating an overall granodioritic composition. The granulite terrain is also characterized by a considerable amount of partial melt generated by dehydration melting. In the center of the granulite area, about 1000 km^2 of hercynite–quartz facies rocks occur, indicating an exceptionally wide outcrop of high-temperature rocks [37]. Peak metamorphic conditions were around 850°C and 5 kbar [19], passing gradually over a distance of 200 km to overlying amphibolite facies rocks with 680°C and 4 kbar [20] as peak conditions. The area is characterized by 42 km of crust, with 25 km of predominantly mafic lower crust [38]. Waters [19,37] and Willner [20] interpret the origin of this belt as stacking of an Andean-type convergent margin, with the high geotherm being produced by magmatic underplating. Penetrative deformation in the entire area is prior to the peak of metamorphism, and related to stacking with a general top to SW (Fig. 8) tectonic movement, with abundant pre- and syn-kinematic intrusions of calcalkaline granitoids [39,40]. Although there is no evidence for a decrease of P at high T preserved in the granulites themselves [37], such a conclusion can be drawn from the amphibolite terrain [20]. The subhorizontal foliation produced by stacking was subsequently refolded to large-scale megafolds of km wavelength (including small-scale steep structures). This is the only retrograde deformation at high temperature and involves relatively small amounts of horizontal shortening, accommodated by some vertical extension [41]. There is no indication of retrograde extensional deformation or later orogenesis contributing to the extremely slow ($\gg$100 Myr) exhumation of the granulites [37]. At and after the peak of metamorphism, the Namaqua granulites were at a depth level of 12–15 km, where the density of the dominant felsic quartz-bearing rocks under this extreme geothermal gradient must have been considerably less than that of the upper crust according to Figs. 1b and 4a. Considering the markedly long period of cooling, generally slow buoyant uprise of high-grade rocks by about 4 km relative to the amphibolite facies terrain (Fig. 7b) to produce the exposed metamorphic zonation seems realistic (Fig. 8).

6. Conclusion

It can be concluded that metamorphic phase transformations proceeding with increasing temperature should be considered as a possible source of gravitational instability of the continental crust when low dP/dT geotherms are characteristic. Thus, low- to medium-pressure granulite facies metamorphism might be 'genetically' related to an increase in the degree of gravitational instabil-

ity within initially stable homogeneously thickened continental crust. Metamorphic phase transformations, partial melting and thermal expansion of minerals can be expected to accompany exponential lowering of the effective viscosity of rocks with increasing temperature. This can lead to the activation of crustal processes of gravitational redistribution (crustal diapirism) that in turn result in significant displacement and complex deformation of metamorphic rocks within the crust (e.g. [4,5,8–10,13,42–44]). This suggests a strong link between external collisional and internal gravitational mechanisms of rock deformation in high-grade metamorphic regions. Since collisional mechanisms should be operative during the early prograde stages of a tectono-metamorphic cycle, causing thickening of the crust and a corresponding increase in radiogenic heat supply, gravitational mechanisms can be expected to dominate during the later thermal peak and retrograde stages, providing an important factor for the exhumation of granulite facies rocks.

Acknowledgements

This work was carried out as part of an RF-RSA scientific collaboration supported by RFBR Grant # 00-05-64939 to T.V.G., by FRD and Gencor grants to D.D.V.R., and by an Alexander von Humboldt Foundation Research Fellowship to T.V.G. We also acknowledge support by the German Research Society through SFB 526. The authors are grateful to J. Connolly, J. Dixon and anonymous reviewers for their valuable suggestions, resulting in substantial improvements to the manuscript, and to B.J. Wood for able editorial support.*[BW]*

References

[1] S.L. Harley, The origin of granulites: a metamorphic perspective, Geol. Mag. 126 (1989) 215–231.
[2] A.B. Thompson, Heat, fluids, and melting in the granulite facies, in: D. Vielzeuf, Ph. Vidal (Eds.), Granulites and Crustal Evolution, NATO ASI Series, Series C, Kluwer, Dordrecht, 1990, pp. 37–58.
[3] F.S. Spear, Metamorphic Phase Equilibria and Pressure–Temperature–Time paths, Min. Soc. America Publication, Washington, DC, 1993, 799 pp.
[4] L.L. Perchuk, P–T-fluid regimes of metamorphism and related magmatism with specific reference to the Baikal Lake granulites, in: S. Daly, D.W.D. Yardley, B. Cliff (Eds.), Evolution of Metamorphic Belts, Geol. Soc. London, Spec. Publ., 1989, pp. 275–291.
[5] H. Ramberg, Gravity, Deformation and Geological Application, Academic Press, London, 1981, 452 pp.
[6] D.L. Turcotte, G. Schubert, Geodynamics: Applications of Continuum Physics to Geological Problems, John Wiley, NY, 1982, 450 pp.
[7] G. Ranalli, Rheology of the Earth, 2nd edn., Chapman and Hall, London, 1995, 413 pp.
[8] L.L. Perchuk, Y.Y. Podladchikov, A.N. Polyakov, P–T paths and geodynamic modelling of some metamorphic processes, J. Metamorph. Geol. 10 (1992) 311–319.
[9] T.V. Gerya, L.L. Perchuk, D.D. Van Reenen, C.A. Smit, Two-dimensional numerical modeling of pressure–temperature–time paths for the exhumation of some granulite facies terrains in the Precambrian, J. Geodyn. 30 (2000) 17–35.
[10] D. Bittner, H. Schmeling, Numerical modeling of melting processes and induced diapirism in the lower crust, Geophys. J. Int. 123 (1995) 59–70.
[11] P.C. England, A.B. Thompson, Pressure–temperature–time paths of regional metamorphism; I, Heat transfer during the evolution of regions of thickened continental crust, J. Petrol. 25 (1984) 894–928.
[12] X. Le Pichon, P. Henry, B. Goffé, Uplift of Tibet: from eclogites to granulites – implications for the Andean Plateau and the Variscan belt, Tectonophysics 273 (1997) 57–76.
[13] T.V. Gerya, L.L. Perchuk, W.V. Maresch, D.D. Van Reenen, C.A. Smit, A.P. Willner, Numerical modeling of the exhumation of Precambrian granulite facies terrains, Ber. Dtsch. Min. Ges. Beih. Eur. J. Mineral. 12 (2000) 59.
[14] R. Bousquet, B. Goffe, P. Henry, X. Le Pichon, C. Chopin, Kinematic, thermal and petrological model of the Central Alps: Lepontine metamorphism in the upper crust and eclogitisation of the lower crust, Tectonophysics 273 (1997) 105–127.
[15] I.K. Karpov, A.I. Kiselev, F.A. Letnikov, Computer Modeling of Natural Mineral Formation, Nedra Press, Moscow, 1976, 256 pp. (in Russian).
[16] C. de Capitani, T.H. Brown, The computation of chemical equilibrium in complex systems containing non-ideal solid solutions, Geochim. Cosmochim. Acta 51 (1987) 2639–2652.
[17] S.V. Sobolev, A.Yu. Babeyko, Modeling of mineralogical composition, density and elastic wave velocities in anhydrous magmatic rocks, Surv. Geophys. 15 (1994) 515–544.
[18] W. Johannes, The significance of experimental studies for the formation of migmatites, in: V.A. Ashworth (Ed.), Migmatites, Blackie, Glasgow, 1985, pp. 36–85.
[19] D.J. Waters, Metamorphic evidence for the heating and cooling path of Namaqualand granulites, in: S. Daly,

D.W.D. Yardley, B. Cliff (Eds.), Evolution of Metamorphic Belts, Geol. Soc. London, Spec. Publ., 1989, pp. 357–363.
[20] A.P. Willner, Pressure–temperature evolution of a low-pressure amphibolite facies terrain in Central Bushmanland (Namaqua Mobile Belt; South Africa), Geol. Surv. Namib. Spec. Publ. 15 (1995) 5–19.
[21] T.J.B. Holland, R. Powell, Internally consistent thermodynamic data set for phases of petrological interest, J. Metamorph. Geol. 16 (1998) 309–344.
[22] T.J.B. Holland, J. Baker, R. Powell, Mixing properties and activity–composition relationships of chlorites in the system $MgO–FeO–Al_2O_3–SiO_2–H_2O$, Eur. J. Mineral. 10 (1998) 395–406.
[23] R. Powell, T.J.B. Holland, Relating formulations of the thermodynamics of mineral solid solutions: Activity modeling of pyroxenes, amphiboles, and micas, Am. Miner. 84 (1999) 1–14.
[24] J. Dale, T.J.B. Holland, R. Powell, Hornblende–garnet–plagioclase thermobarometry: a natural assemblage calibration of the thermodynamics of hornblende, Contrib. Mineral. Petrol. 140 (2000) 353–362.
[25] S. McLennan, Continental crust, Encycl. Earth Sci. 1 (1992) 1085–1098.
[26] B.W.D. Yardley, An Introduction to Metamorphic Petrology, Earth Sciences Series, Longman, Singapore, 1989, 248 pp.
[27] A.D. Nozkhin, O.M. Turkina, Geochemistry of Granulites, Institute Geol. Geophys. Russian Acad. Sci. Press, Novosibirsk, 1993, 224 pp. (in Russian).
[28] R.L. Rudnick, D.M. Fountain, Nature and composition of the continental crust: a lower crustal perspective, Rev. Geophys. 33 (1995) 267–309.
[29] R. Kretz, Symbols for rock-forming minerals, Am. Miner. 68 (1983) 277–279.
[30] R.G. Berman, Internally-consistent thermodynamic data for minerals in the system $Na_2O–K_2O–CaO–MgO–FeO–Fe_2O_3–Al_2O_3–SiO_2–TiO_2–H_2O–CO_2$, J. Petrol. 29 (1988) 445–522.
[31] T.V. Gerya, K.K. Podlesskii, L.L. Perchuk, V. Swamy, N.A. Kosyakova, Equations of state of minerals for thermodynamic databases used in petrology, Petrology 6 (1998) 511–526.
[32] B. Schott, H. Schmeling, Delamination and detachment of a lithospheric root, Tectonophysics 296 (1998) 225–247.
[33] W.F. Brace, Limits on lithospheric stress imposed by laboratory experiments, J. Geophys. Res. 85 (1980) 6248–6252.
[34] N.L. Carter, M.C. Tsenn, Flow properties of continental lithosphere, Tectonophysics 136 (1987) 27–63.
[35] L.L. Perchuk, T.V. Gerya, D.D. Van Reenen, C.A. Smit, A.V. Krotov, P–T paths and tectonic evolution of shear zones separating high-grade terrains from cratons: examples from Kola Peninsula (Russia) and Limpopo Region (South Africa), Mineral. Petrol. 69 (2000) 109–142.
[36] C.A. Smit, D.D. Van Reenen, T.V. Gerya, D.A. Varlamov, A.V. Fed'kin, Structural–metamorphic evolution of the Southern Yenisey Range of Eastern Siberia: implications for the emplacement of the Kanskiy granulite Complex, Mineral. Petrol. 69 (2000) 35–67.
[37] D.J. Waters, Thermal history and tectonic setting of the Namaqualand granulites, Southern Africa: clues to Proterozoic crustal development, in: D. Vielzeuf, Ph. Vidal (Eds.), Granulites and Crustal Evolution, NATO ASI Series, Series C, Kluwer, Dordrecht, 1990, pp. 243–256.
[38] R.W.E. Green, R.J. Durrheim, The seismic structure of the Namaqualand Metamorphic Complex, Geocongress 88 Durban, Extended Abstract, 1988, pp. 171–174.
[39] G. Van Aswegen, D. Strydom, W.P. Colliston, H.E. Praekelt, A.E. Schoch, H.J. Blignault, B.J.V. Botha, S.W. van der Merwe, The structural-stratigraphic development of part of the Namaqua Metamorphic Complex, South Africa – An example of Proterozoic major thrust tectonics, in: A. Kröner (Ed.), Proterozoic Lithospheric Evolution, Am. Geophys. Union Geodyn. Ser., NY, 1987, pp. 207–216.
[40] J.M. Moore, A Comparative Study of Metamorphosed Supracrustal Rocks from the Western Namaqualand Metamorphic Complex, Ph.D. thesis, University of Cape Town, Cape Town, 1986, 370 pp.
[41] A.F.M. Kisters, E.G. Charlesworth, R.L. Gibson, C.R. Anhaeusser, Steep structure formation in the Okiep Cooper District, South Africa: bulk inhomogeneous shortening of a high-grade metamorphic granite–gneiss sequence, J. Struct. Geol. 18 (1996) 735–751.
[42] V.V. Beloussov, Geotectonics, Nedra Press, Moscow, 1989, 381 pp. (in Russian).
[43] R.B. Weinberg, H. Schmeling, Polydiapirs: multiwavelength gravity structures, J. Struct. Geol. 14 (1992) 425–436.
[44] P.H.G.M. Dirks, Crustal convection: evidence from granulite terrains, Centennial Geocongress, Extended Abstracts, Geol. Soc. South Africa, 1995, pp. 673–676.